Technical Report Prepared for: European Energy	Document Number: EEN-01-01-TRP-001-1

Omø Syd Offshore Wind Farm Ornithology Impact
Bird Modelling - Final Report

EP Consult Energies

EUROPEAN ENERGY

INTELLIGENT
ENGINEERING

Revision History

Rev.	Date	Description	By	Checked	Approved
1	17-Jun-21	Update following additional client comments	SP	MN	MHL
0	10-Jun-21	Update following additional client comments	SP	MN	MHL
C	08-Jun-21	Update following client review	SP	MN	MHL
B	31-May-21	Client Issue	SP	MN	MHL
A	28-May-21	Internal review	SP	MN	

EPConsult Energies
Østerbrogade 212
2100 Copenhagen Ø
Denmark

T: +45 5359 3555
T: +44 20 7582 5555
www.ep-consult.dk
info@ep-consult.co.uk

Table of Contents

Table of Tables

Table of Figures

1   Introduction

The proposed Omø Syd wind farm lies within an area proposed as a Special Protection Area/Bird Protection Area (SPA) for birds under the EU Birds Directive. This report investigates the possible exclusion of the wind farm site from the SPA and whether that exclusion could be offset through alternative extensions to the SPA, to provide quantitative evidence to assist in the overall assessment process. Common Eider and Red-necked Grebe both occur in the area in internationally important numbers (>1% of the flyway population), and hence meet the qualifying thresholds for designation.

The aim of this study is to compare the numbers of the two qualifying species (Common Eider *Somateria mollissima* and Red-necked Grebe *Podiceps grisegena*) within three Special Protection Area (SPA) option areas: (a) designation as currently proposed, (b) an alternative designation with the wind farm and a 1km buffer excluded from SPA; and (3) the exclusion proposed in (b) plus additional extension options. The study area for this work was defined to include all of the proposed SPA and its surrounds (see Figure 1-1), where baseline bird and environmental data were available.

The work had three specific phases:

- Phase 1 - Integration of all relevant bird survey data to estimate bird densities in grid squares within the area surveyed.

- Phase 2 - Spatial modelling with environmental factors (including seabed habitat type, water depth, seabed topography, distance from shore and distance from potential sources of disturbance (e.g. main shipping channels, designated hunting areas) - to understand the factors affecting bird distribution and predict bird densities in unsurveyed areas.

- Phase 3 - Application of the model to test the SPA alternatives.
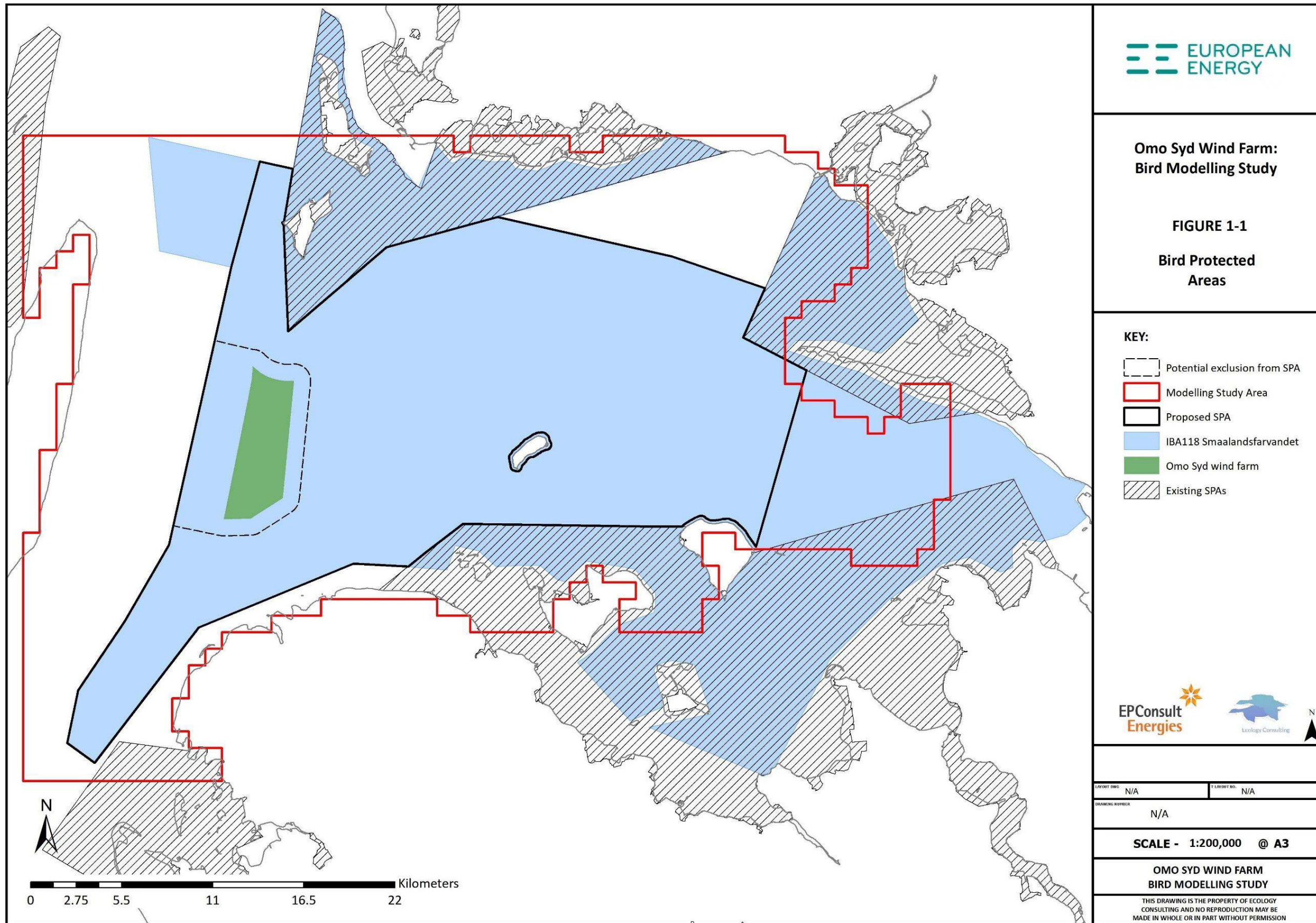
Figure 1-1: Bird Protected Areas

EPConsult Energies
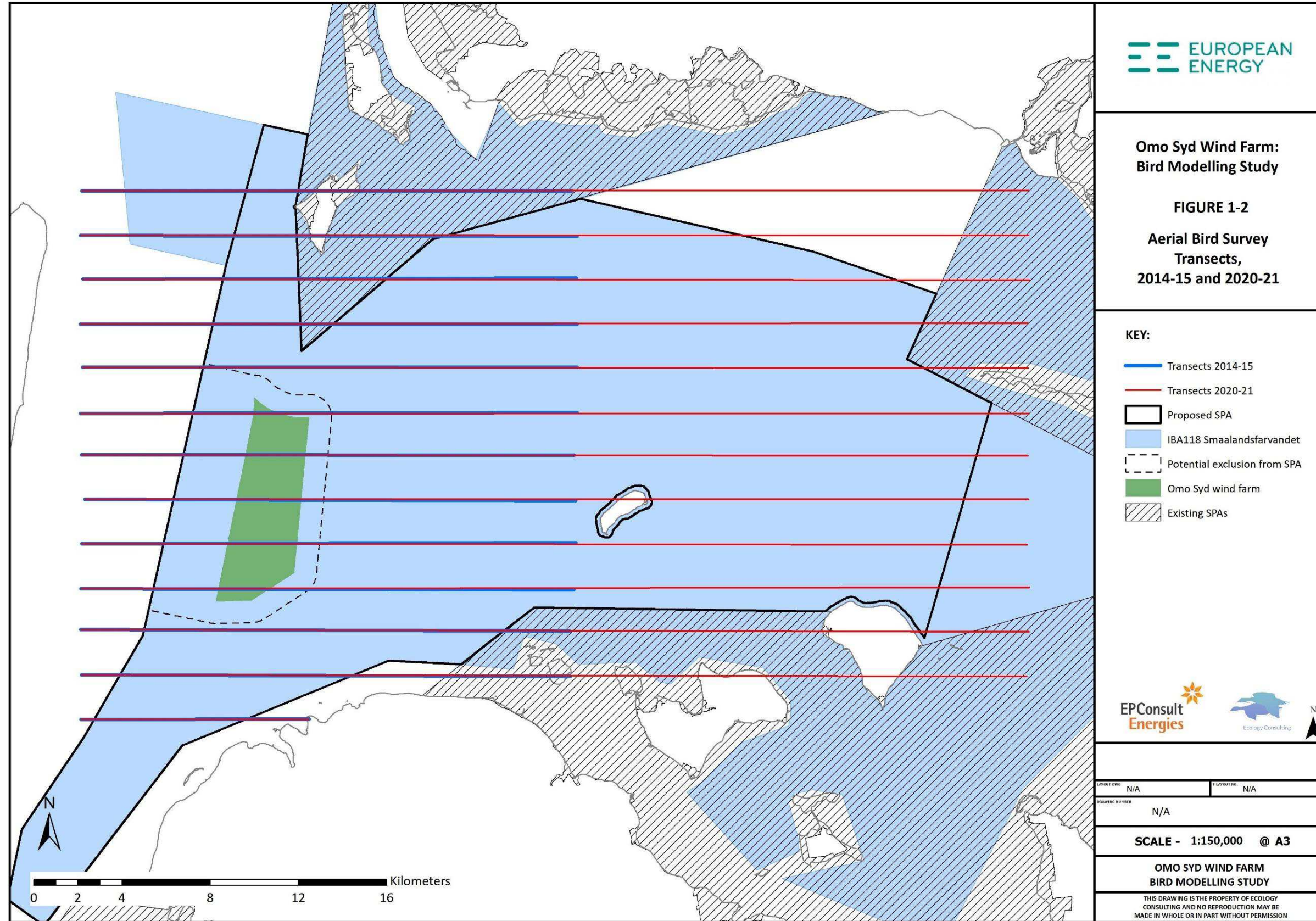
Omo Syd Wind Farm: Bird Modelling Study

FIGURE 1-2

Aerial Bird Survey Transects, 2014-15 and 2020-21

KEY:

— Transects 2014-15
— Transects 2020-21
☐ Proposed SPA
IBA118 Smaalandsfarvandet
Potential exclusion from SPA
Omo Syd wind farm
Existing SPAs

EPConsult Energies   Ecology Consulting

| LAYOUT DWG | N/A | LAYOUT NO. | N/A |
| DRAWING NUMBER | | N/A | |

SCALE - 1:150,000   @ A3

**OMO SYD WIND FARM
BIRD MODELLING STUDY**

THIS DRAWING IS THE PROPERTY OF ECOLOGY CONSULTING AND NO REPRODUCTION MAY BE MADE IN WHOLE OR IN PART WITHOUT PERMISSION

Figure 1-2: Aerial Bird Survey Transects, 2014-15 and 2020-21

2   Phase 1 Baseline Data: Birds

The first phase of the work was to collate and process the available bird survey data to be used in the spatial modelling exercise. This included:

- Assessing the coverage of the baseline bird surveys in relation to the maximum extent of the proposed SPA, to identify the gaps (in space and time).

- Determining an appropriate size for a grid square overlay of the SPA, optimised for the scale of data available on birds and habitats/environmental data. A grid square of 1x1km was chosen for the modelling in line with the spatial scale of the study and the bird surveys. Grid squares were centred on the survey transects.

- Collation of the raw bird survey data and survey effort (transect routes, dates of surveys).

- Standardising the data for survey effort.

- Taking into account the seasonality of use of the area.

- Calculation of an overall value of bird density for grid squares covered by the baseline surveys – expressed as mean count per unit area (with confidence intervals).

Two survey programmes have been undertaken by the developer of the Omø Syd wind farm. Both were carried out by BioConsult, an international leader in seabird aerial survey techniques. The survey transects are shown in Figure 1-2. Surveys comprised:

- 2020-21 - survey area included wind farm site plus buffer and most of the pSPA (a total area of about 1,050km^2). Nine surveys were carried out over the whole of this area, at approximately 3-4 weeks intervals between October 2020 and April 2021.

- 2014-15 - carried out to inform the original project EIA. These covered a reduced survey area of 550km^2 but the same survey methodology and transects as the 2020-21 surveys (within the reduced area). Figure 1-2 shows the transect routes followed in each year. Five surveys were carried out in total, between October and December 2014, and in March and April 2015.

All surveys were carried out as visual aerial surveys to maintain consistency over time and allow comparison with the Danish national monitoring scheme (NOVANA), using a standard survey protocol. Two observers were used, each covering one side of the aircraft. Flight altitude during surveys was standardised at 78m (250 feet) at a cruising speed approximately 185 km (100 knots, Kahlert *et al*. 2000), to enable rapid approach to birds sitting on the sea, causing minimal disturbance but still allowing time for identification. Birds were recorded to three standardised distance intervals out from the track-line taken by the aircraft: 49-174m (band A), 175-459m (band B) and 460m-1km (band C). Observers could not observe a band of width 49 m on either side of the flight track since this was obscured by the body of the plane. The limits of each band were determined using a clinometer which enabled the measurement of predetermined angles below the horizontal measured abeam (at 78m altitude, the 49m cut-off is an angle of 60° from the horizontal, 174m is 25° and 459m represents 10° declination). Position along the transect was recorded by noting the precise time (to the nearest second) at which the bird or flock of birds is perpendicular to the observer using watches synchronised with GPS. The time at which each observation along the transect was made can be converted into a position by interpolating the GPS data and placing observations into a predetermined distance from the track-line according to the band in which the bird was recorded.

No correction was made for diving/submerged birds, so the values should be treated as minimum estimates, but this would not be expected to affect the proportionate distributions (and hence the key conclusions of the report).

The visual aerial surveys raised two specific data issues:

- Declining detectability from the survey platform - birds were recorded to distance bands from the survey aircraft, but this was effectively only two bands for these surveys and so few birds were recorded in band C - only 3% of Common Eider records and zero Red-necked Grebe were recorded in band C during 2020-21, and 6.5% of Common Eider in 2014-15. No Grebes were again recorded in band C in 2014-15.

- o Whilst it would be possible to adopt a simple approach and use only the Band A data to calculate bird densities (Diederichs *et al* 2002), this would mean discarding large amounts of data that were recorded in Band B. Options were therefore explored to maximise the use of the data, use the principles of distance sampling to estimate correction factors to incorporate the Band B data as well as that from Band A (though with effectively only two bands DISTANCE software itself could not be used). Distance correction factors were calculated for Band B for each survey, standardising to the same overall density as Band A. Data from Band C was not used in the density estimates (as this comprised only a very small proportion of the data set and was insufficient to generate reliable estimates).

- Identification to species level - whilst Common Eiders were readily recognisable from a survey plane, it is difficult to separate Red-necked Grebe from another grebe species that occurs frequently in this area, Great Crested Grebe. Whilst some observers were able to do this confidently, others recorded only to 'grebe species'.

  - o Further examination of the survey data showed that there was a marked seasonal pattern of occurrence of confirmed identifications of these species, that could be used to classify the unidentified records. Overall, from the 2020-21 data, 91% of confirmed Great Crested Grebe records occurred before 15 November, whilst 94% of Red-necked Grebe were seen after this date, so this was used as a cut-off to classify the unidentified records to species.

Older data from the NOVANA monitoring and from the Smålandsfarvandet Offshore Wind Farm proposal (which did not go ahead) were also collated for this study but time constraints (and issues with data temporal and spatial coverage) meant that they could not be included explicitly in the modelling work. There may, however, be an opportunity for further model testing and refinement using those data during the EIA updating exercise. For this current exercise, the 2020-21 data have been used for the initial model building as the most up-to-date baseline and with widest coverage, then that model has been tested with the 2014-15 data over the reduced area that those earlier surveys covered.

3 Phase 1 Baseline Data: Environment

Data on the environmental factors that could affect Common Eider and Red-necked Grebe distribution across the study area were collated and are summarised in Table 3-1. They included:

- seabed sediment type;
- water depth;
- seabed slope;
- seabed current speed;
- seabed suitability index for filter-feeding bivalves (DHI model - Skov *et al.* 2012)
- distance from shore;
- shipping activity (AIS 2016 all-vessel shipping data);
- hunting and hunting-free areas.

All were available across the whole of the study area.

Table 3-1: Summary of environmental data included in the spatial modelling analysis

Environmental Data	Source	Comments
Seabed sediment type	GEUS download	
Index of seabed suitability for filter-feeding bivalves	DHI model (Skov *et al.* 2012)	Derived from a DHI hydrodynamic/nutrient flow/ecological productivity model that incorporates data on tide, salinity, temperature and nutrient run-off and loadings (Skov *et al.* 2012)
Water Depth	COWI	Bathymetry by 50m grid
Seabed slope;	COWI	Calculated from bathymetry data to 50m grid
Seabed current speeds	DHI	
Shipping activity	AIS data 2016 (all vessels)	https://www.soefartsstyrelsen.dk/sikkerhed-til-soes/sejladsinformation/download-data/datasaet
Distance from shore		Calculated from coastline
Designated hunting areas and shooting-free refuges in the region;		https://miljoegis.mim.dk/spatialmap?profile=miljoegis-skovdrift

It had been intended to investigate the effect of hunting disturbance as an additional variable in the modelling, but as no quantitative data were available on hunting levels or locations within the proposed SPA, this was not investigated further.

4 Baseline Data Description

4.1 Seabed Sediment Type

The seabed sediment types across the study area are shown in Figure 4-7. The total areas of each habitat within the proposed SPA are given in Table 4-1.

Table 4-1: Seabed sediment type within the study area and within the proposed SPA.

Seabed sediment type	Area (study area) km²	% of study area
Mud and muddy sand	72	11%
Muddy sand	140	21%
Sand	127	19%
Till/diamicton	338	50%

4.2 Water Depth

The study area bathymetry is shown in Figure 4-8, with deeper areas shown in blue and shallower in red. The range of water depths across the survey area is shown in the histogram in Figure 4-1. Most of the study area was relatively shallow, with only a small area of deeper water, predominantly in the western part of the area (Figure 4-1).
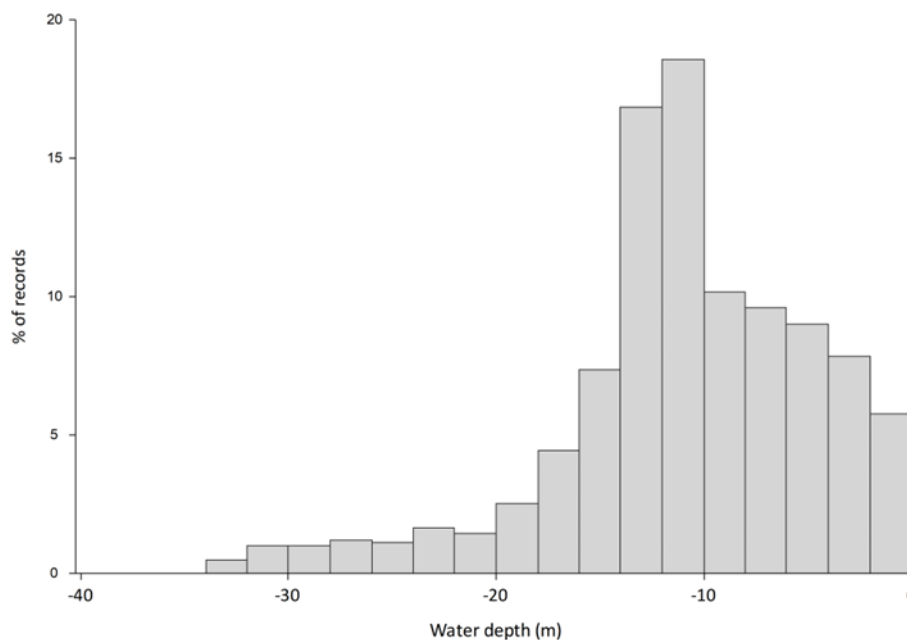
Figure 4-1: Water Depths within the study area

4.3 Seabed slope

Seabed slope was calculated on a 50m grid basis by COWI for input into the modelling. Slopes across the study area are mapped in Figure 4-9. The large majority of the seabed across the study area was flat, with only a small area of areas of higher slope (Figure 4-2).
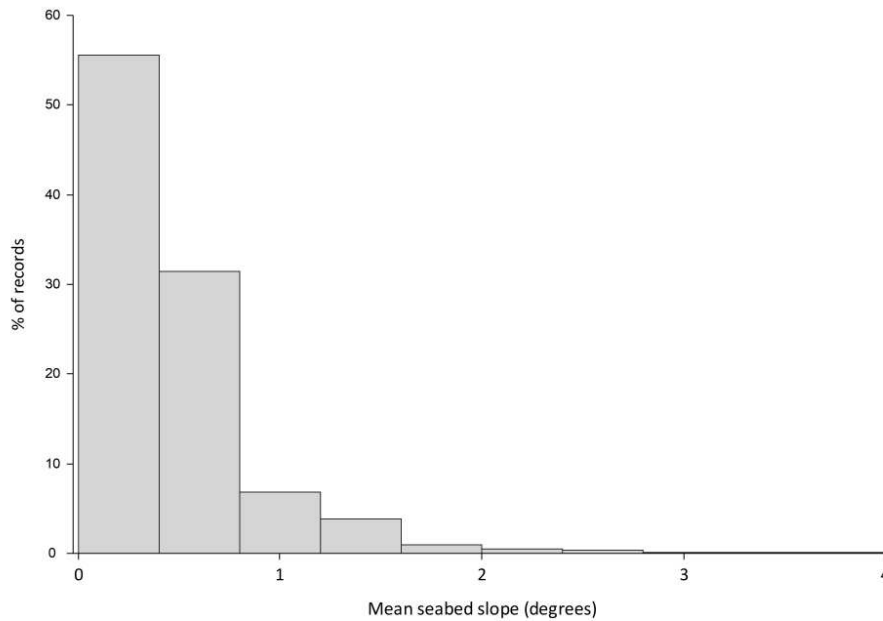
Figure 4-2: Seabed slope within the study area

4.4 Seabed current speed

Figure 4-10 shows the distribution of seabed current speeds within the study area, and these are summarised in Figure 4-3. Most areas had low current speeds, with areas of higher speed largely restricted to the western part of the survey area.
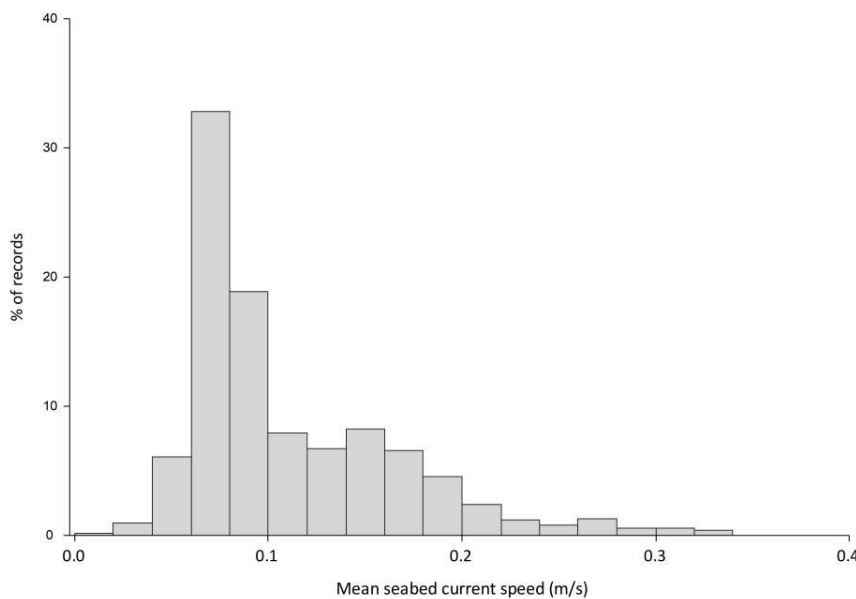
Figure 4-3: Seabed current speed within the study area

4.5   Seabed suitability index for filter-feeding bivalves (DHI)

The seabed suitability index for filter-feeding bivalves from the DHI model (Skov *et al*. 2012) is mapped across the study area in Figure 4-11 and summarised in Figure 4-4. Large parts of the study were classed as very low suitability, with two separate zones of higher suitability (shown in Figure 4-11 as red/orange areas).
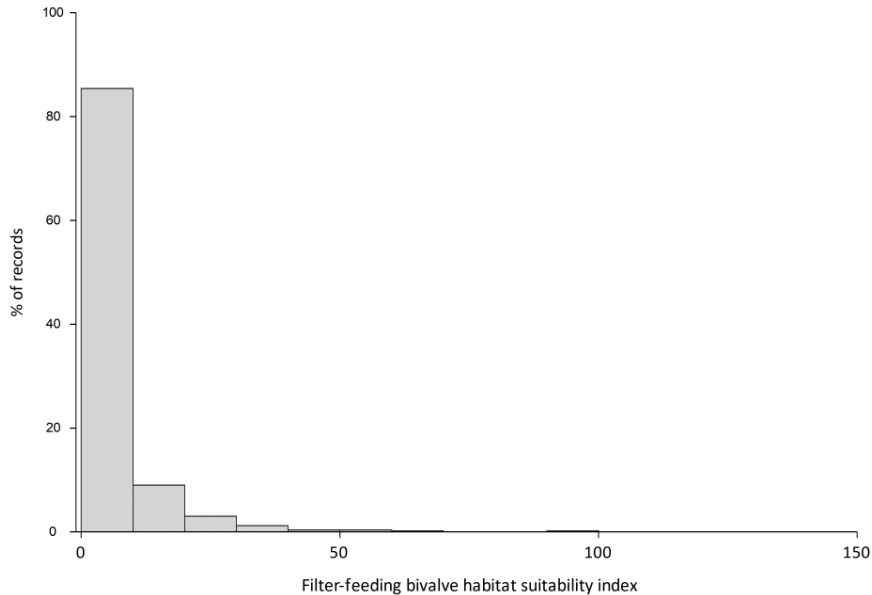
Figure 4-4: Filter-feeding bivalve suitability index (source: DHI) within the study area

4.6   Distance from shore

Figure 4-5 summarises the distribution of distances from the shore across the study area. The most frequent category was within 1km of the shore, and the majority within 5km, up to a maximum of 10km.
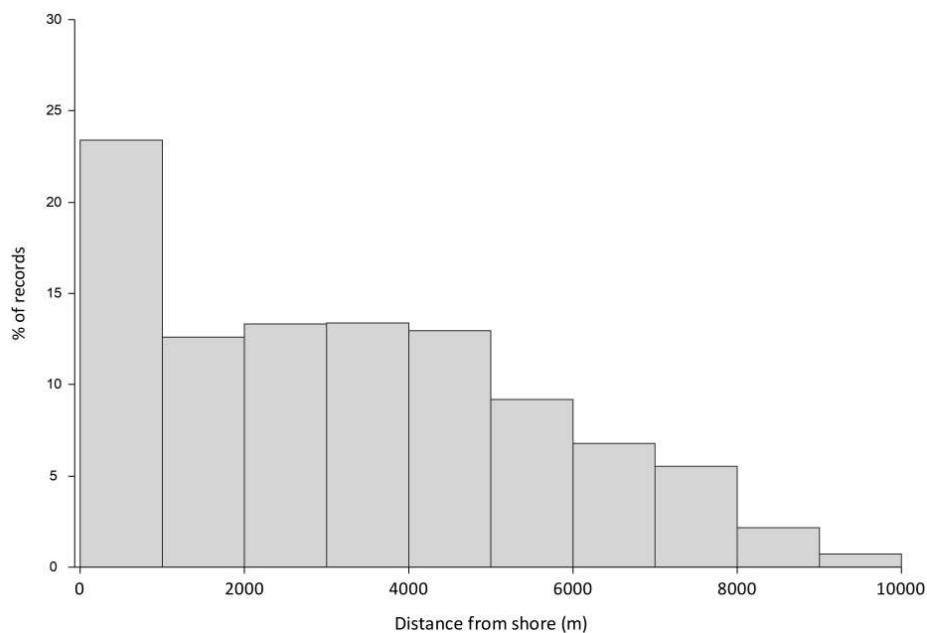
Figure 4-5: Distance from the shore within the study area.

4.7   Shipping activity (AIS 2016 all-vessel shipping data)

Shipping activity within the study area (as determined from the 2016 AIS data) was concentrated within the main shipping channel on the western edge (Figure 5-15 and Figure 4-6), with much less within the proposed SPA.
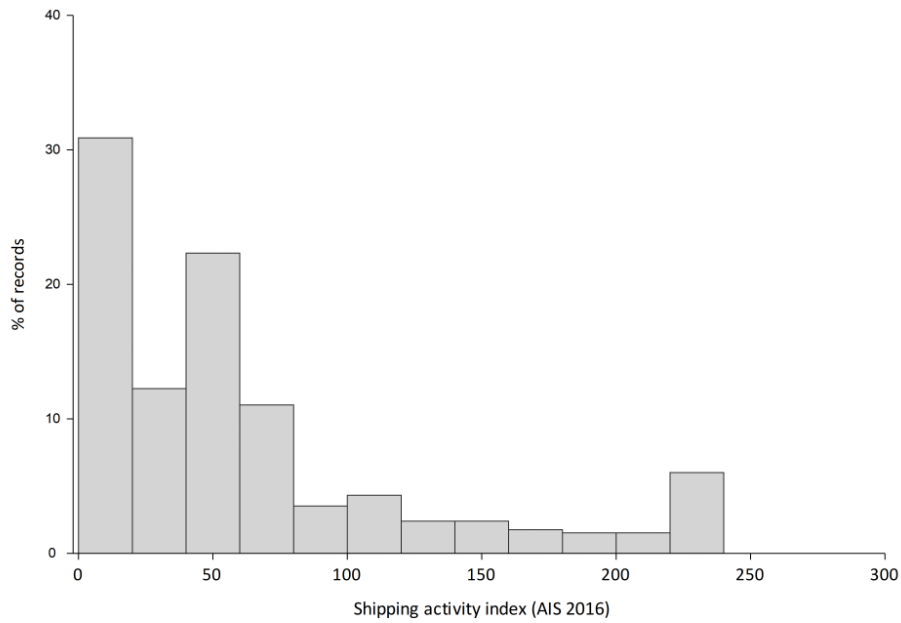
Figure 4-6: Shipping activity levels (source: AIS 2016) within the study area
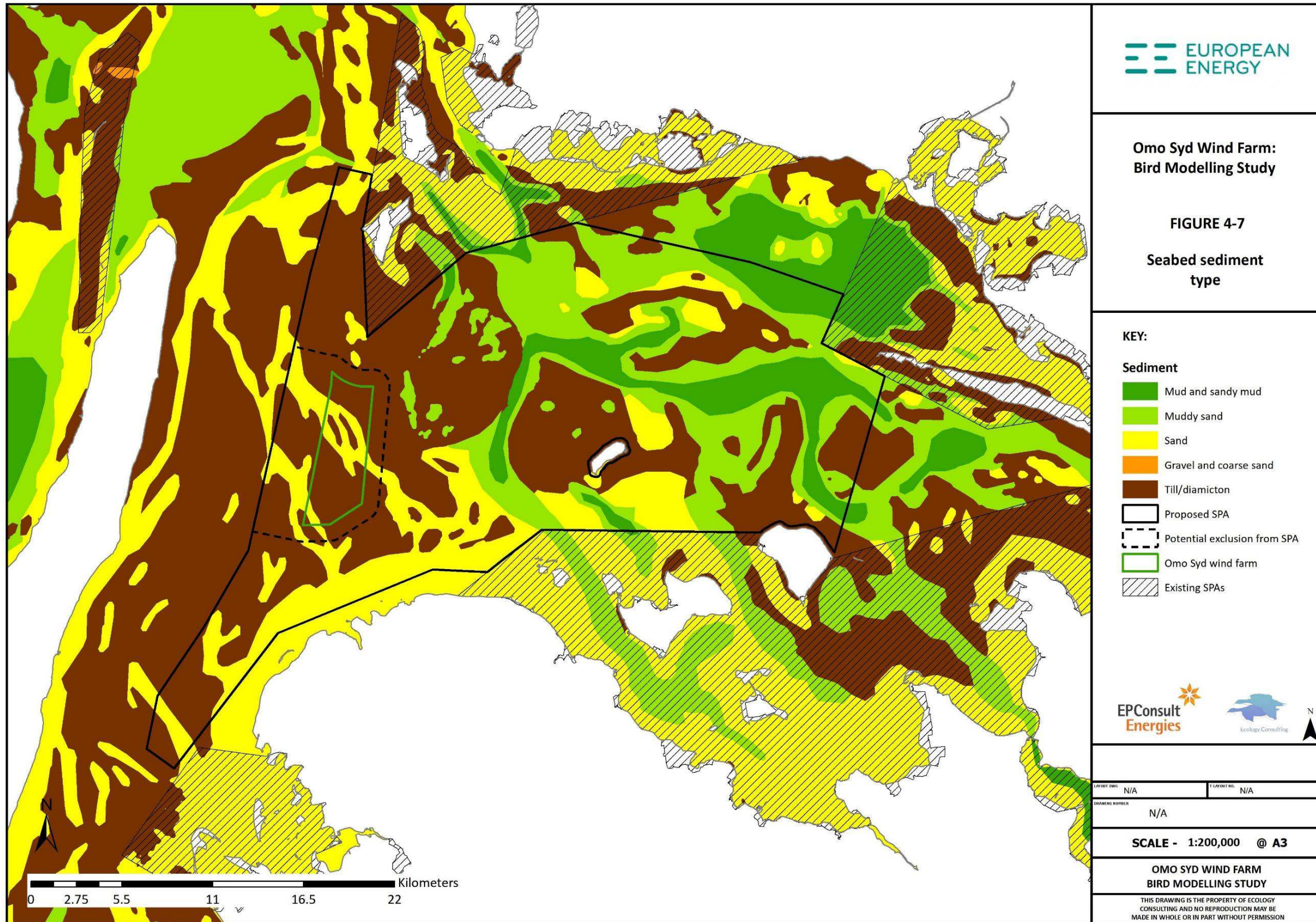
Figure 4-7: Seabed Sediment Type

**Omo Syd Wind Farm:
Bird Modelling Study**

FIGURE 4-8

Bathymetry

KEY:

Proposed SPA

Potential exclusion from SPA

Omo Syd wind farm

Existing SPAs

Red (shallower)
- Blue (deeper)

[scale to add]

SCALE - 1:200,000 @ A3

OMO SYD WIND FARM
BIRD MODELLING STUDY

THIS DRAWING IS THE PROPERTY OF ECOLOGY
CONSULTING AND NO REPRODUCTION MAY BE
MADE IN WHOLE OR IN PART WITHOUT PERMISSION
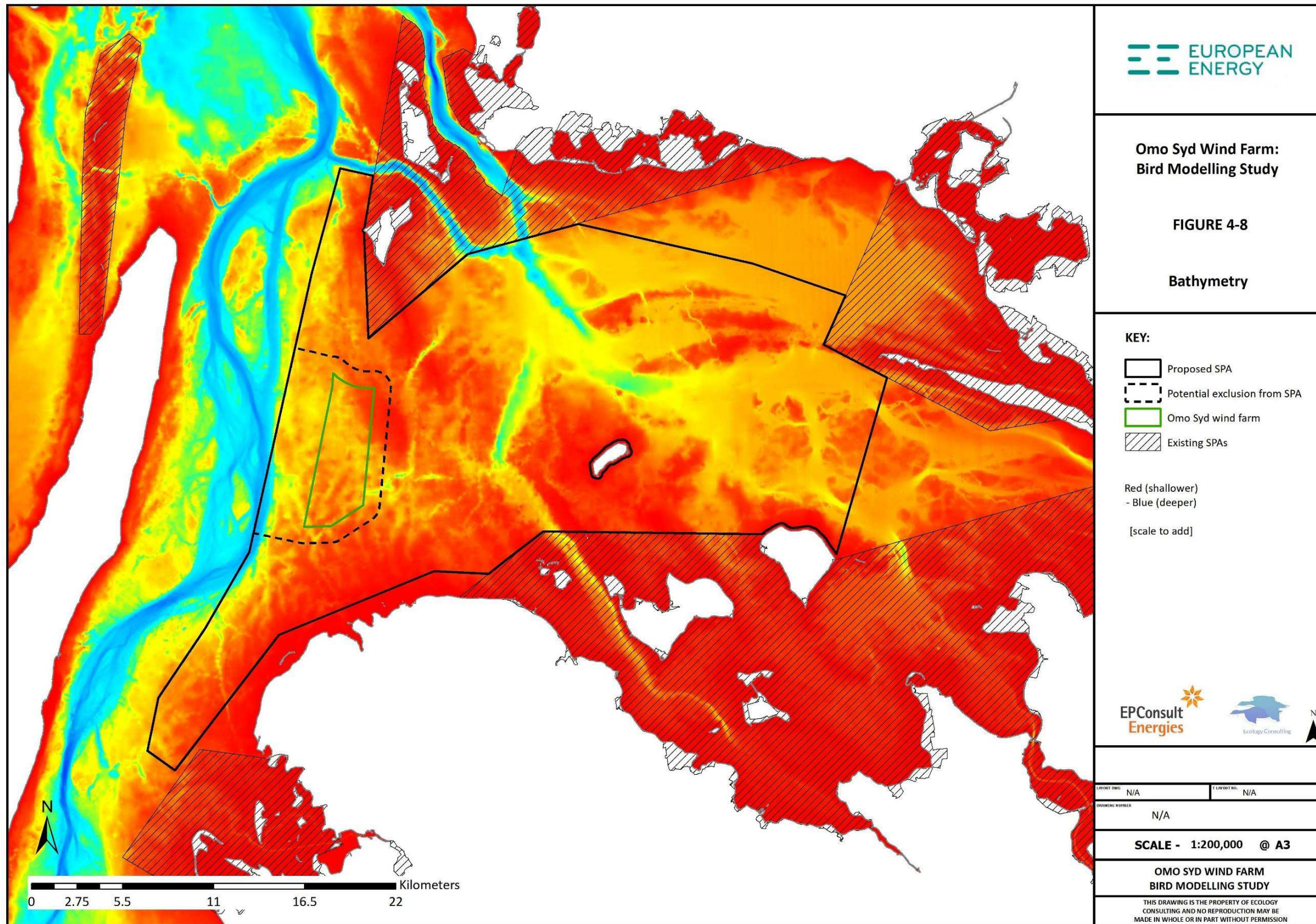
Figure 4-8: Bathymetry

Figure 4-9: Seabed Slope (degrees)
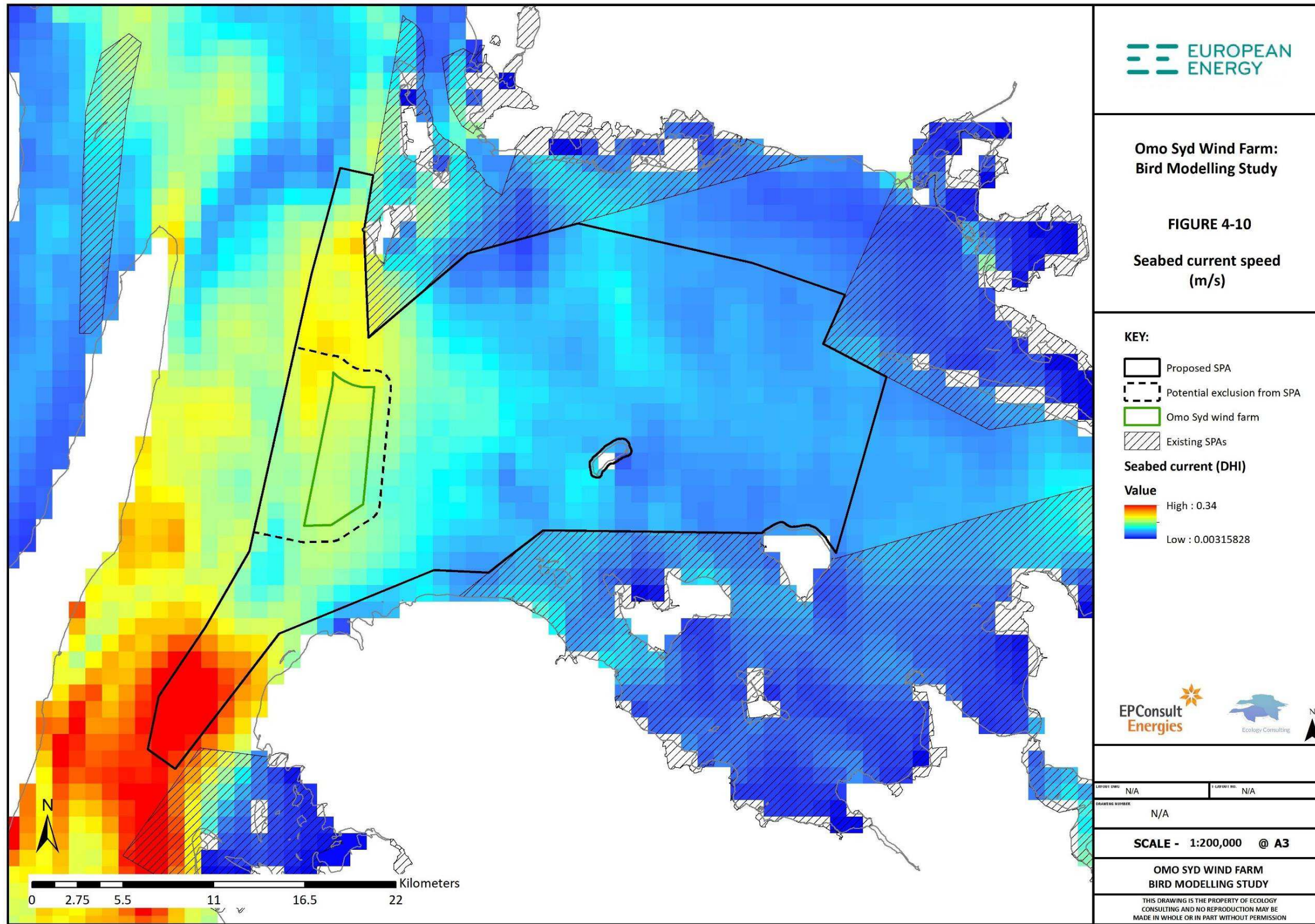
Figure 4-10: Seabed Current Speed (m/s)
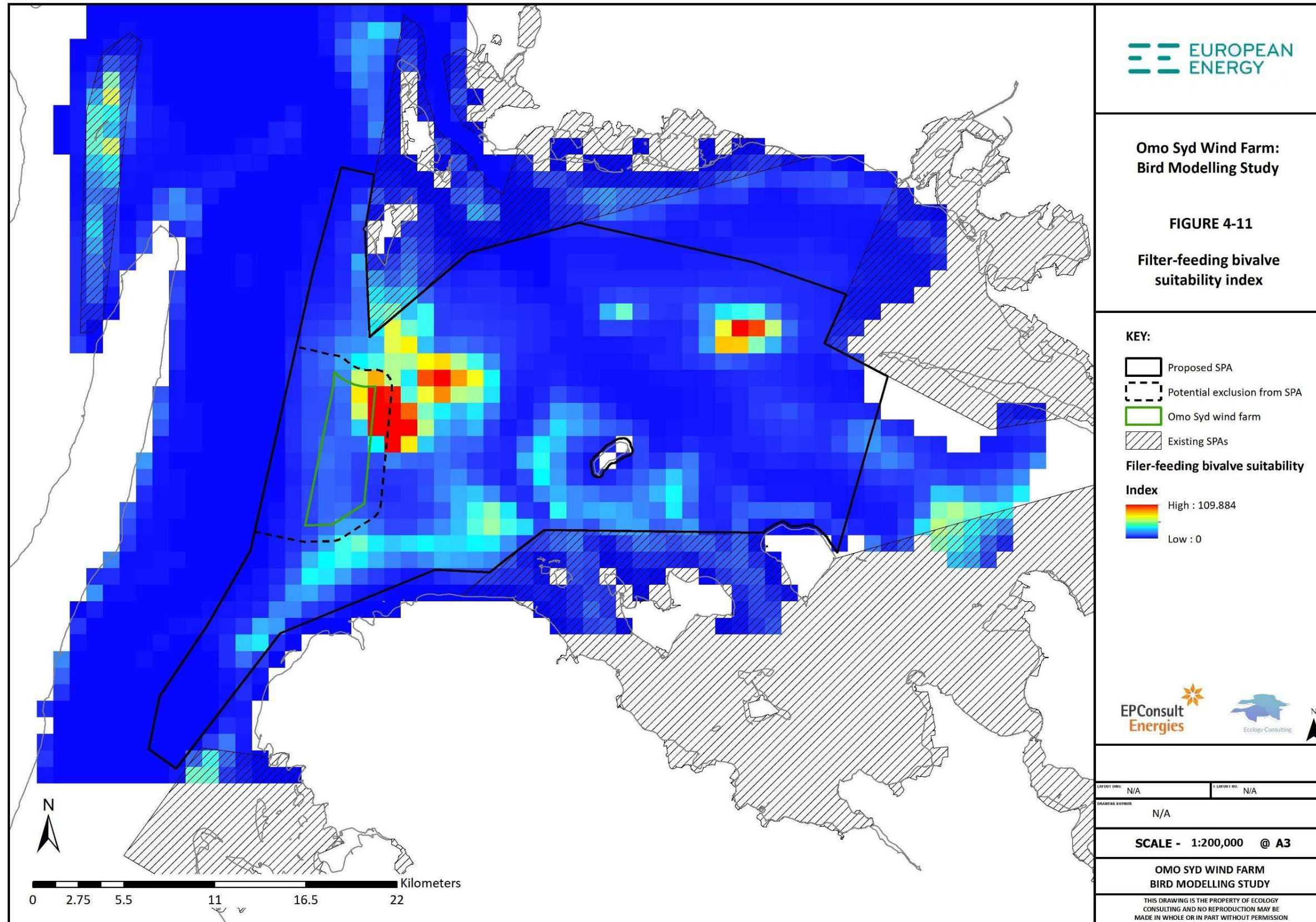
Figure 4-11: Filter Feeding Bivalve Suitability Index
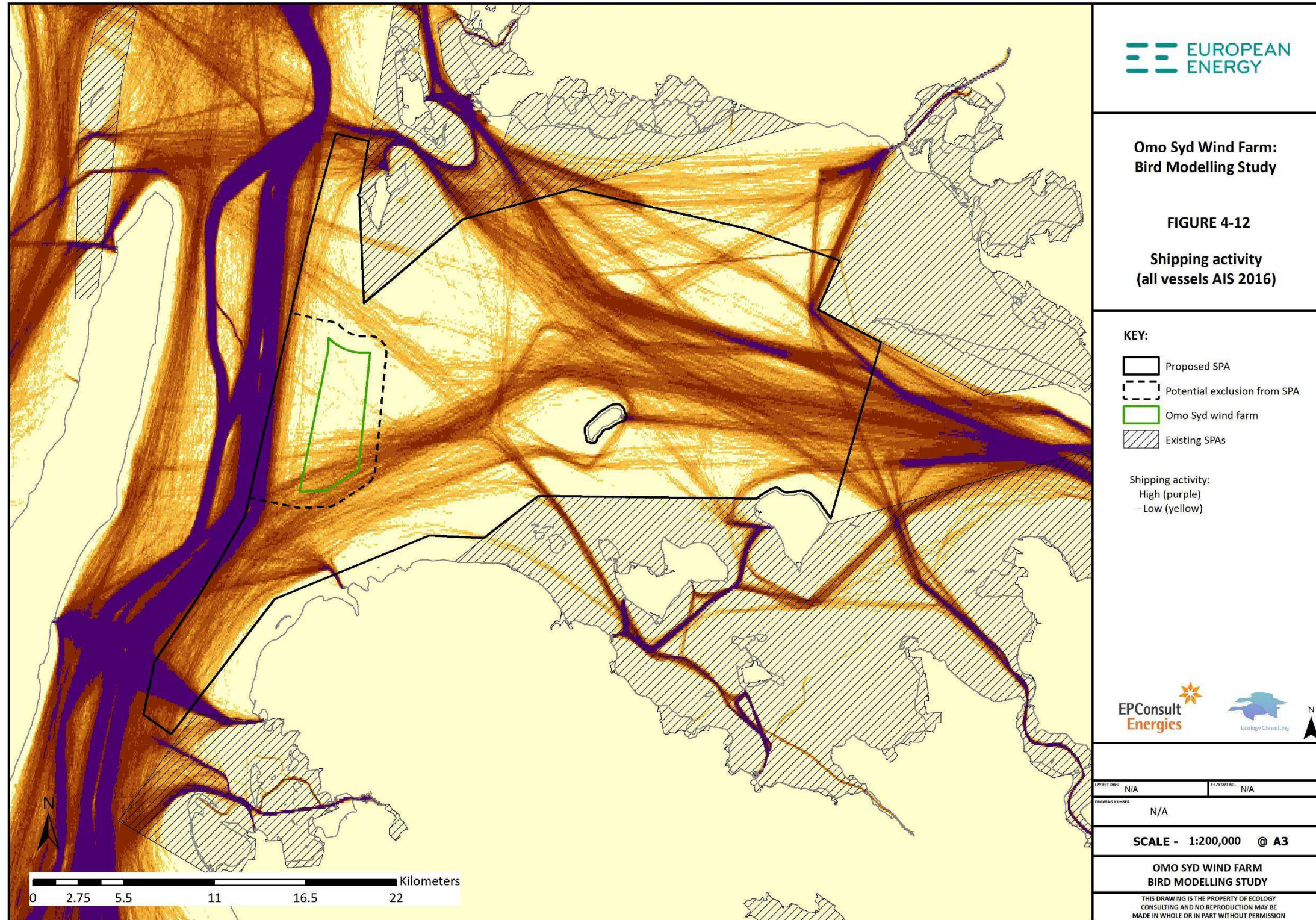
Figure 4-12: Shipping Activity (All Vessels AIS 2016)

5 Phase 2 Developing the Spatial Model

The first stage of the modelling was an initial exploration of the bird densities of each of the two key species (Common Eider and Red-necked Grebe) and each environmental variable.

Figure 5-1 shows the mean (+ standard error) Common Eider density in each of the four main seabed sediment types. The till/diamicton areas held the highest Eider densities, and the mud/sandy mud the lowest, i.e., there were mode Eiders on hard substrates. Common Eider densities were statistically significantly different between sediment types (Kruskal Wallis test: H=15.6, p=0.0014, n=509).
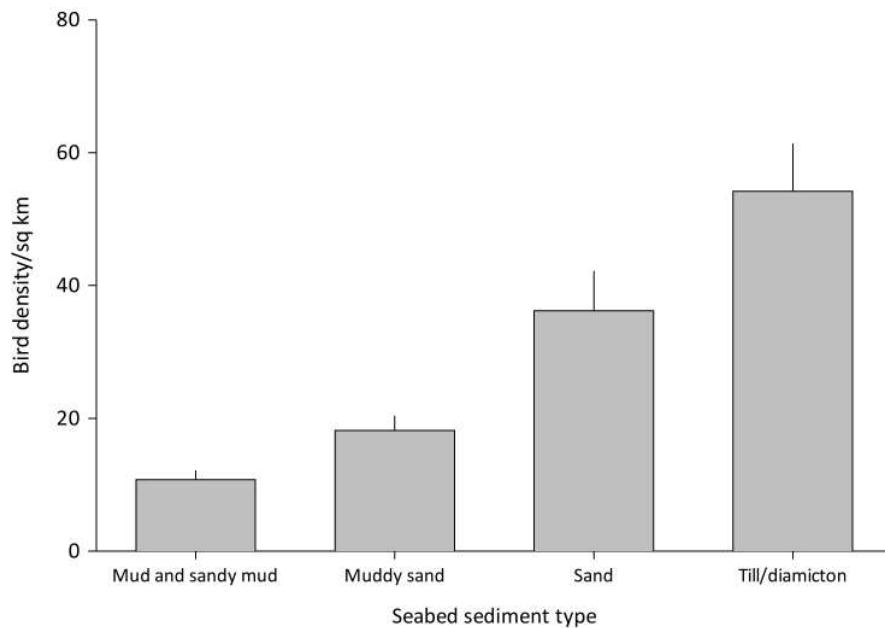
Figure 5-1: Common Eider density across seabed sediment types

There was no clear relationship between Red-necked Grebes density and seabed sediment type (Figure 5-2), with no statistically significant difference (Kruskal Wallis test: H=6.7, p=0.08, n=509).
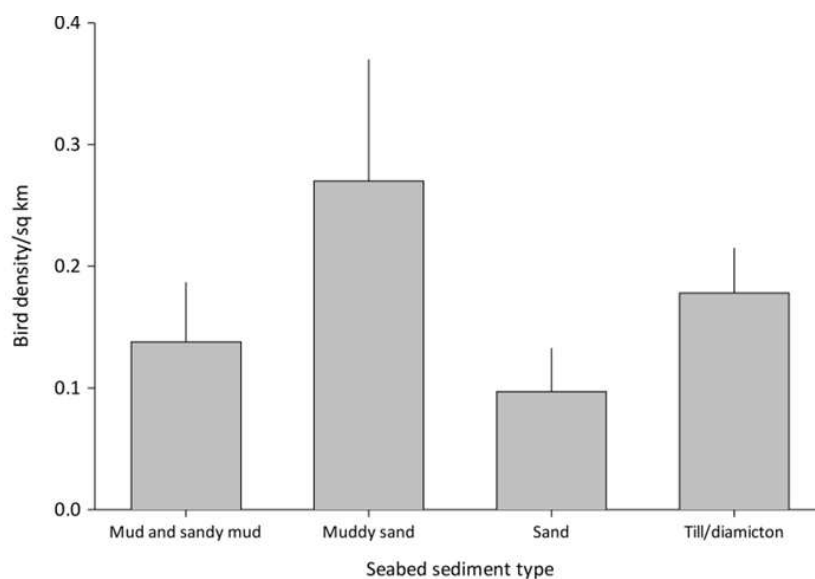
Figure 5-2: Red-necked Grebe density across seabed sediment types

5.1 Water depth

Common Eider densities were higher in shallower water (<10m depth) and lowest below 20m (Figure 5-3). This difference was statistically significant (Kruskal Wallis test: H = 140.4, p<0.0001, n = 509).
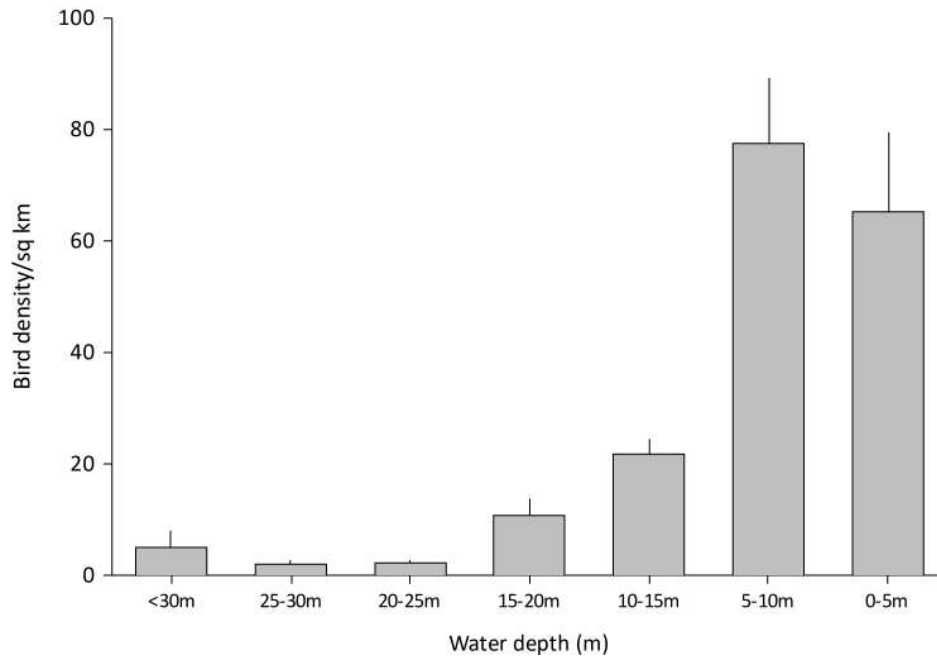
Figure 5-3: Common Eider density and water depth.

Red-necked Grebes were found at reduced density in the shallowest waters (0-5m), and there were no records at all from deeper waters (more than 20m) (Figure 5-4). This difference was statistically significant (Kruskal Wallis test: H = 27.5, p=0.0001, n = 509).
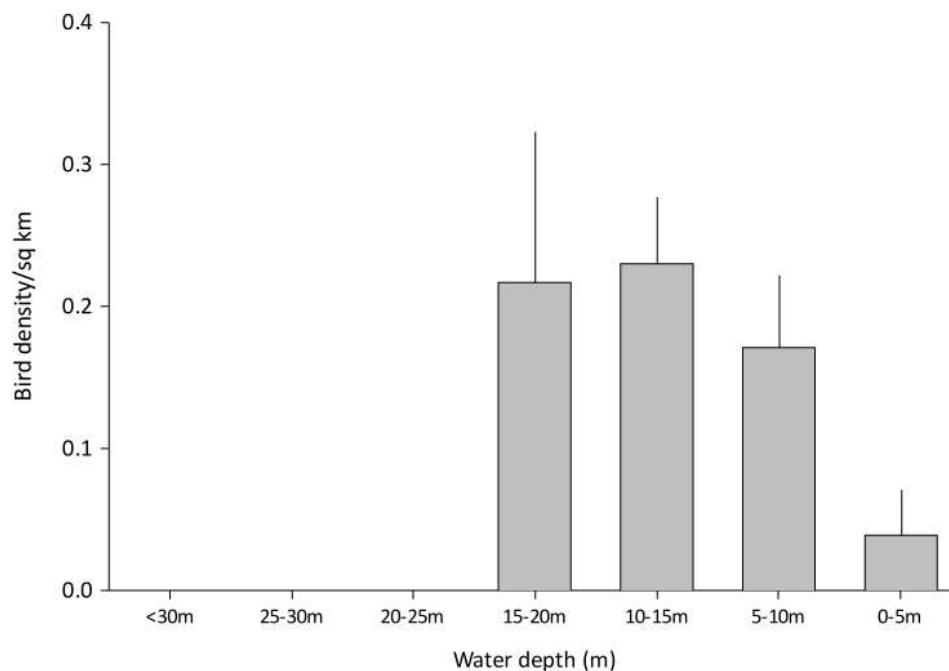
Figure 5-4: Red-necked Grebe density and water depth

5.2   Seabed slope

There was a trend for higher Common Eider densities where seabed slopes were shallower, but this was only a weak relationship. Densities in the 0.25-0.5 degree mean slope zone were significantly higher than those in both flatter and more sloping areas (Kruskal Wallis test: H = 49.6, p<0.0001, n = 509).
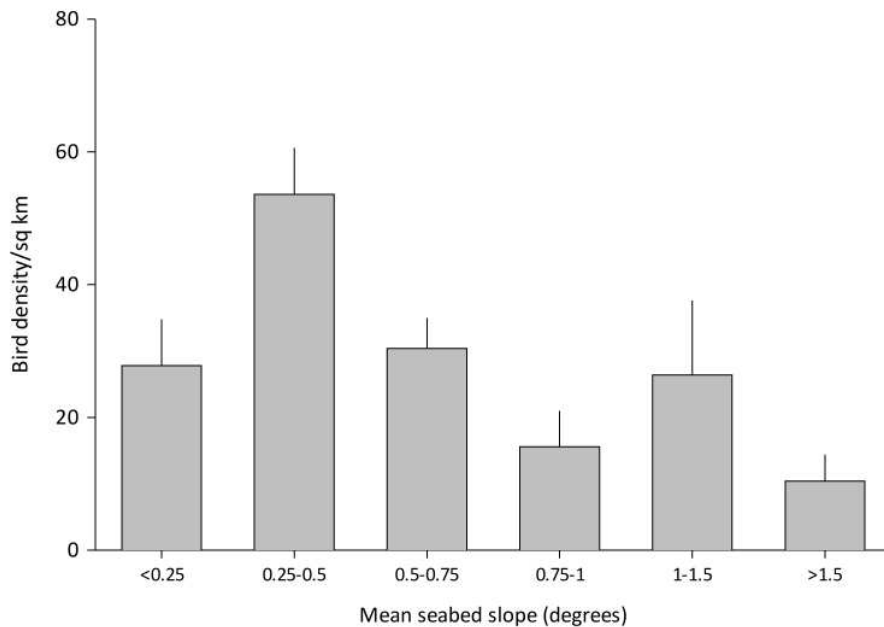
Figure 5-5: Common Eider density and seabed slope

Red-necked Grebe density was also highest in the 0.25 - 0.5 degree class (Figure 5-6), and this was statistically significant (Kruskal Wallis test: H = 12.5, p=0.028, n = 509).

Figure 5-6: Red-necked Grebe density and seabed slope

5.3 Seabed current speed

Common Eider density was generally higher in areas of higher seabed current speed (possibly as a result of the effect of current on food availability/feeding conditions (Kruskal Wallis test: H = 12.5, p=0.028, n = 509), Figure 5-7.
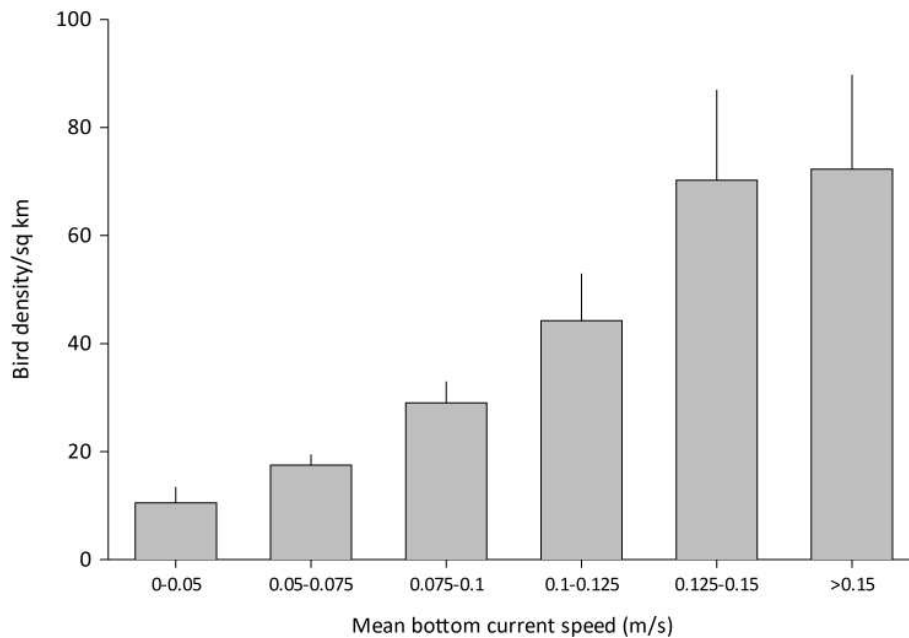
Figure 5-7: Common Eider density and mean bottom current speed

Red-necked Grebe density was generally similar across the range of seabed current speed, though with the notable exception of the mid-range speed class which was significantly higher (Kruskal Wallis test: H = 14.2, p=0.015, n = 509), Figure 5-8.
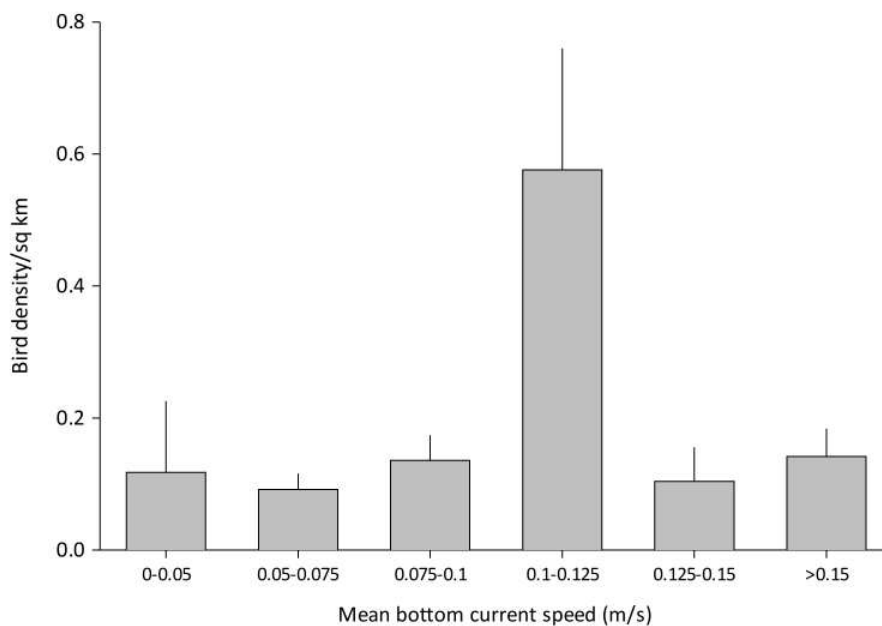
Figure 5-8: Red-necked Grebe density and mean bottom current speed

5.4 Seabed suitability index for filter-feeding bivalves (DHI model, Skov *et al.* 2012)

Common Eider density was higher in areas with higher DHI filter-feeding bivalve habitat suitability index values (Figure 5-9), a result that was highly statistically significant (Kruskal Wallis test: H = 161.9, p<0.0001, n = 509), and one that would be expected given that filter-feeding bivalves such as mussels would be likely to form an important part of the Common Eider diet.
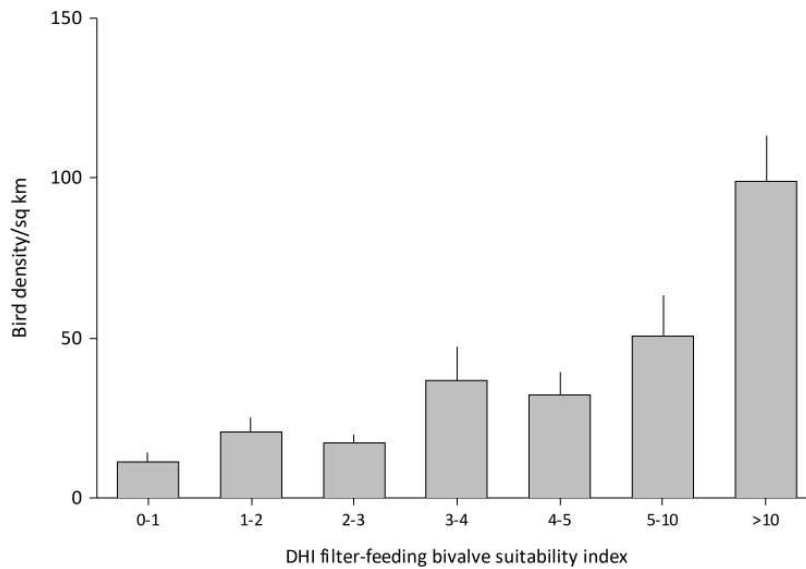
Figure 5-9: Common Eider density and DHI filter-feeding bivalve habitat suitability index

Red-necked Grebe density did not show any clear trends with the DHI filter-feeding bivalve habitat suitability index at lower values (Figure 5-10), with no significant difference between classes (Kruskal Wallis test: H = 8.4, p=0.21, n = 509) (though this would be expected given that this species feeds predominantly on fish).
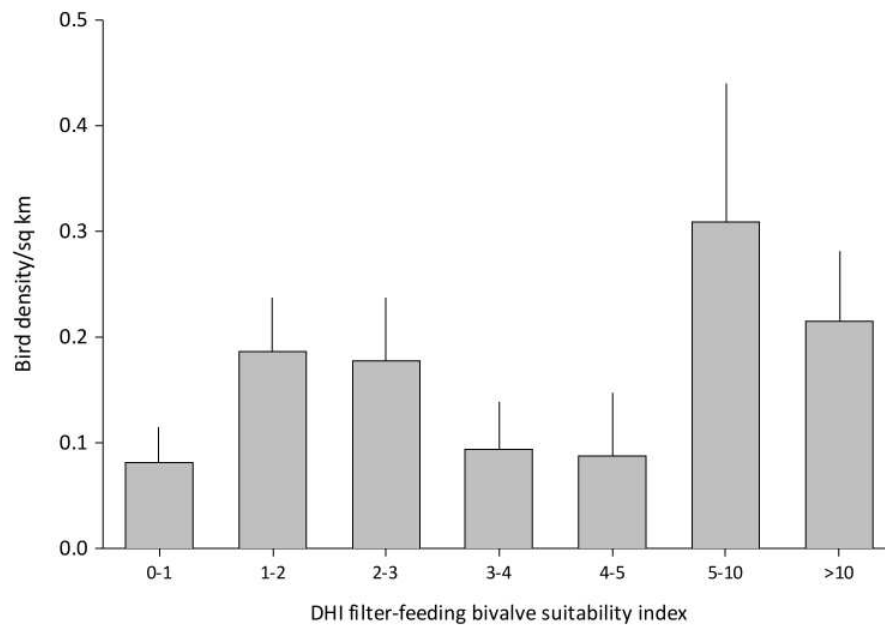
Figure 5-10: Red-necked Grebe density and DHI filter-feeding bivalve habitat suitability index

5.5 Distance from shore

Common Eider densities were higher within 3km of the shore, and also, to a lesser extent in the further (>7km from shore) zone (Figure 5-11). Differences were statistically significant (Kruskal Wallis test: H = 48.0, p<0.0001, n = 509).
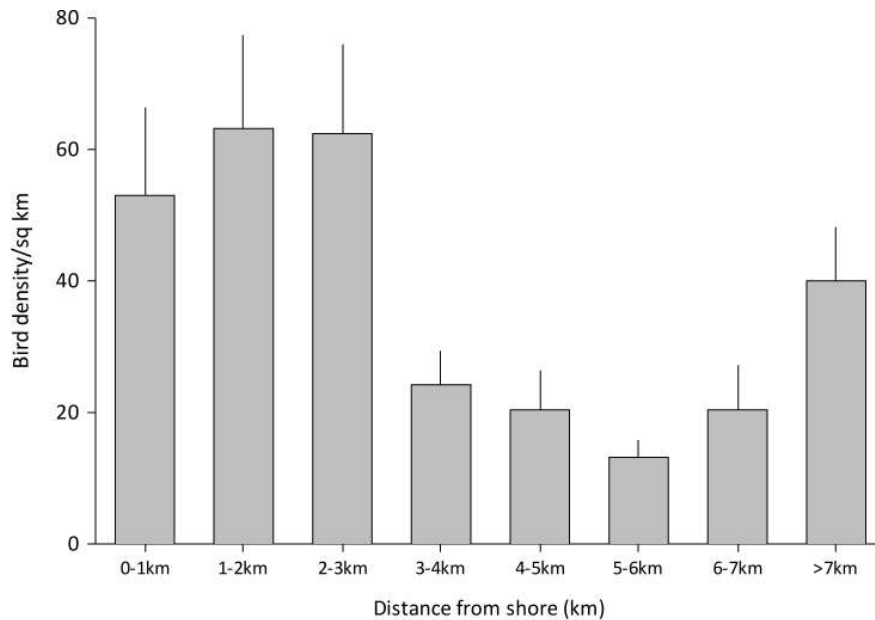
Figure 5-11: Common Eider density and distance from the shore

Red-necked Grebe densities were generally higher further from the shore (Figure 5-12). Differences were statistically significant (Kruskal Wallis test: H = 25.1, p=0.0007, n = 509).
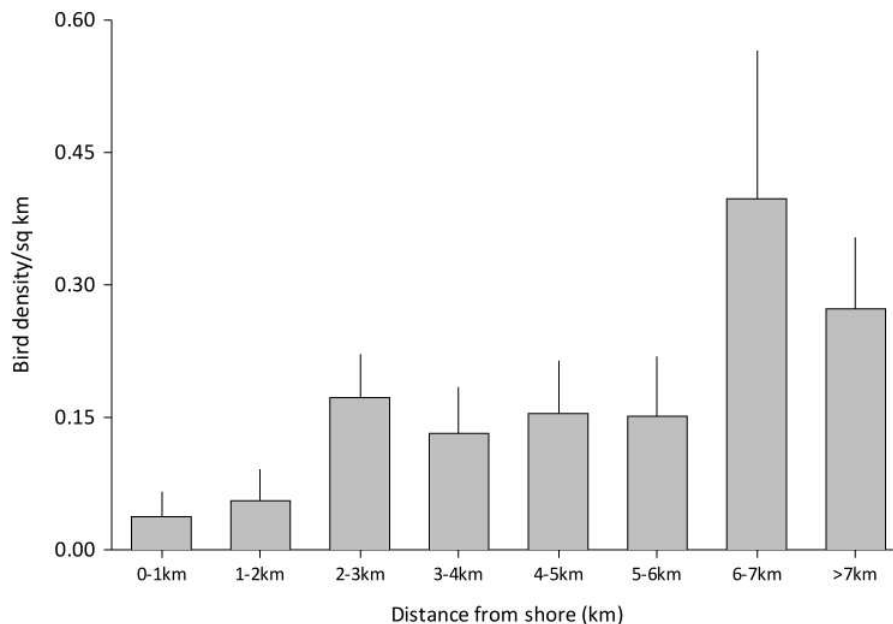
Figure 5-12: Red-necked Grebe density and distance from the shore.

5.6 Shipping activity (AIS 2016 all-vessel shipping data)

Common Eider densities were generally higher in areas of lower shipping activity, particularly in comparison with the highest shipping level (Figure 5-13). Differences were statistically significant (Kruskal Wallis test: H = 61.9, p<0.0001, n = 509).
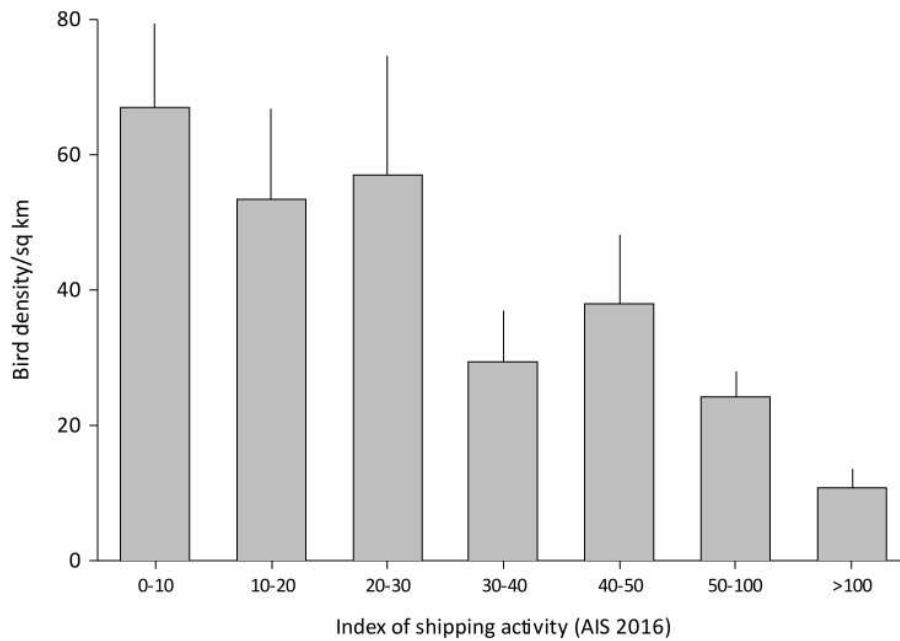
Figure 5-13: Common Eider density and shipping activity index (AIS 2016)

Higher Red-necked Grebe densities were generally found in the mid-range of shipping activity, with fewer at both lower and higher shipping levels (Figure 5-14), but these differences were not statistically significant (Kruskal Wallis test: H = 7.1, p=0.31, n = 509).
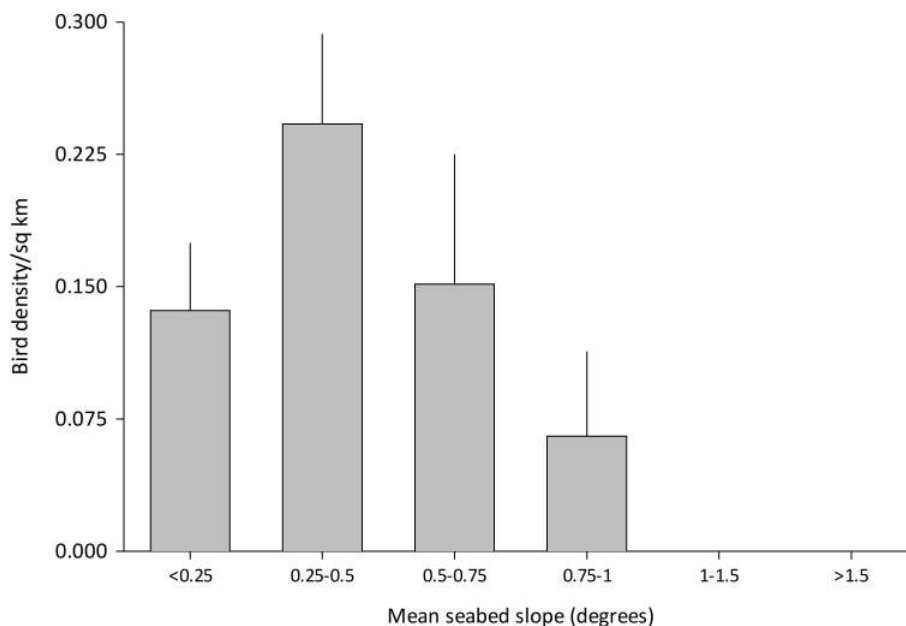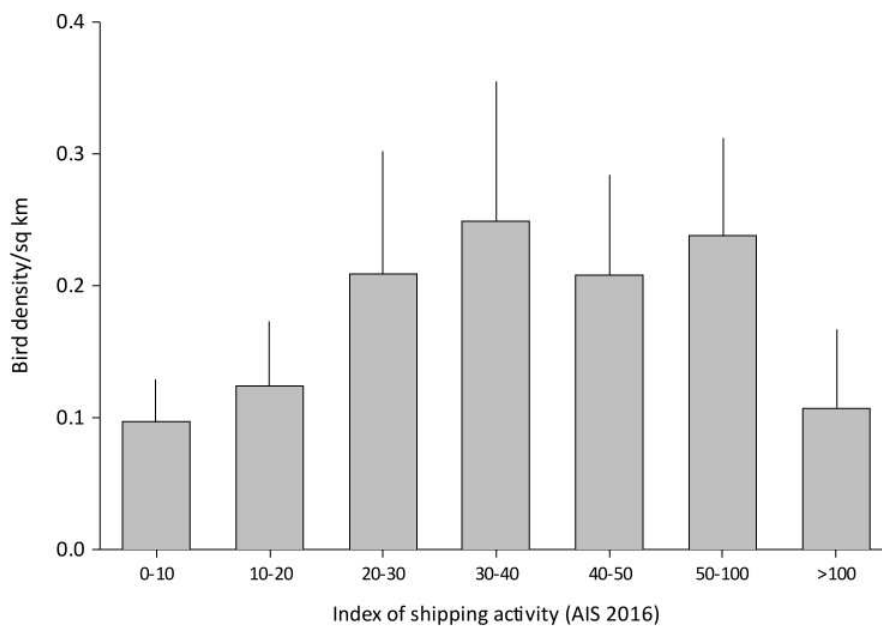

Figure 5-14: Red-necked Grebe density and shipping activity index (AIS 2016)

5.7   Spatial Autoregressive (SAR) Modelling

Spatial Autoregressive Modelling (StataCorp 2021) was used to analyse the bird and environmental data to investigate how Common Eider and Red-necked Grebe abundance was related to these explanatory environmental variables. It enabled the location of each grid square to be included in the modelling to take into account any spatial autocorrelation in the data.

Table 5-1 summarises the results of the SAR for Eider. The model was highly statistically significant overall (with a pseudo-r2 of 0.295, and p<0.0001), with the main environmental variables associated with Common Eider density being the DHI filter-feeding bivalve suitability index (strong positive association; coefficient = 1.32, p=0.005), and distance from the shore (with higher Common Eider densities further from the shore; coefficient = -0.0047, p=0.015).

Table 5-1: Summary of the results of the Spatial Autoregressive Modelling for Common Eider

```
Spatial autoregressive model                    Number of obs =      509
GS2SLS estimates                                Wald chi2(10) = 150.96
                                                Prob > chi2   = 0.0000
                                                Pseudo R2     = 0.2954
```

EI_mean_2021	Coefficient	Std. err.	z	P>|z|	[95% conf. interval]	
EI_mean_2021						
Depth_mean	.7369312	.7817558	0.94	0.346	-.795282	2.269144
Slope_mean	2.554448	8.091822	0.32	0.752	-13.30523	18.41413
DHIFilterFeed_mean	1.322938	.4742779	2.79	0.005	.3933707	2.252506
Current_mean	345.9383	225.5702	1.53	0.125	-96.17116	788.0477
ShoreDistance	-.0046661	.0019229	-2.43	0.015	-.0084348	-.0008973
AIS2016_mean	-.0284401	.047201	-0.60	0.547	-.1209523	.0640721
SedimentClass						
Muddy sand	-2.935428	3.362433	-0.87	0.383	-9.525675	3.654819
Sand	-16.95449	12.11959	-1.40	0.162	-40.70846	6.799479
Till/diamicton	-10.1745	8.404718	-1.21	0.226	-26.64744	6.298449
_cons	7.409122	5.804013	1.28	0.202	-3.966533	18.78478
W_contig						
EI_mean_2021	.6254558	.1658303	3.77	0.000	.3004343	.9504773
e.EI_mean_2021	-.415968	.1706669	-2.44	0.015	-.750469	-.0814669

```
Wald test of spatial terms:        chi2(2) = 14.23      Prob > chi2 = 0.0008
```

Note: 'EI_mean2021' = mean Common Eider density derived from the 2020-21 survey data; 'Depth_mean' = Mean sea depth; 'Slope_mean = Mean seabed slope; 'DHIFilterFeed_mean' = mean filter-feeding bivalve suitability index (DHI); 'Current_mean' = mean bottom current speed; 'ShoreDistance' = ditnace of central point of grid square to shore; 'AIS2016_mean' = mean shipping activity (AIS 2016 data, all vessels), 'SedimentNo' = seabed habitat type, with classes given and tested against 'Mud and sandy mud' baseline; W_contig details the spatial correlation matrix.

The SAR results for Red-necked Grebe are shown in Table 5-2. There was a much weaker relationship between grebe density and the environmental data than there was for Common Eider (with a pseudo-r2 value of only 0.033), though the analysis did still identify a statistically significant relationship between grebe density and the DHI filter-feeding bivalve suitability index (a weak negative association; coefficient = -0.00704, p=0.004). The data for Red-necked Grebes were statistically problematic as well, as they contained a high proportion of zero values (82% of surveyed grid squares held zero r Red-necked Grebes).

Table 5-2: Summary of the results of the Spatial Autoregressive Modelling for Red-necked Grebe

```
Spatial autoregressive model                    Number of obs =      509
GS2SLS estimates                                Wald chi2(10) =    63.60
                                                Prob > chi2   =   0.0000
                                                Pseudo R2     =   0.0332
```

RNG_mean_2021	Coefficient	Std. err.	z	P>|z|	[95% conf. interval]	
RNG_mean_2021						
Depth_mean	.0100775	.0098401	1.02	0.306	-.0092088	.0293638
Slope_mean	-.0195533	.0774475	-0.25	0.801	-.1713476	.132241
DHIFilterFeed_mean	-.0070359	.002432	-2.89	0.004	-.0118026	-.0022692
Current_mean	.7270698	.6814129	1.07	0.286	-.6084749	2.062614
ShoreDistance	9.14e-06	.0000123	0.74	0.459	-.000015	.0000333
AIS2016_mean	.0007597	.0007378	1.03	0.303	-.0006864	.0022058
SedimentClass						
Muddy sand	.0530355	.0892147	0.59	0.552	-.1218222	.2278932
Sand	-.1312287	.0951864	-1.38	0.168	-.3177906	.0553332
Till/diamicton	-.0702287	.0897957	-0.78	0.434	-.246225	.1057675
_cons	-.3485771	.1064883	-3.27	0.001	-.5572903	-.1398639
W_inv						
RNG_mean_2021	3.233291	.7353747	4.40	0.000	1.791983	4.674599
e.RNG_mean_2021	-1.557351	1.34616	-1.16	0.247	-4.195777	1.081074

```
Wald test of spatial terms:        chi2(2) = 19.67      Prob > chi2 = 0.0001
```

5.8 Model Validation

The outputs from these models were tested initially against the 2020-21 data, to compare the model predictions with the observed densities of each species. A further independent test of the predictions was carried out with the 2014-15 data, to see how the model predictions compared with the observed densities in that winter (only the 2020-21 data were used in the model development), though this could only be carried out for the reduced survey area that was covered in that year.

Both the 2014-15 and the 2020-21 survey data were strongly correlated with the predicted densities for Common Eider (r_s = 0.44 and r_s = 0.49 respectively, p<0.0001 and n=509 in both years). The predicted values from the model matched well to the observed survey data, validating the model predictions.

For Red-necked Grebe the SAR model predictions were a poor fit for both the 2014-15 (r_s = -0.089, p=0.05, n=509) and the 2020-21 data (r_s = 0.082, p=0.07, n=509), showing no statistically significant correlation. The predicted values did not match well to the observed survey data, indicating that the model predictions were not reliable for this species. This means that the model cannot be used to produce reliable predictions of Red-necked Grebe densities outside the areas surveyed.

As a reliable model has been produced for Common Eider, this has been used to construct a density surface model, using a combination of the observed data from the 2020-21 surveys (that covered a wider survey area) and filling the gaps with the model-predicted densities. The results are shown in Figure 5-15.

The lack of a statistically reliable model for Red-necked Grebe using the environmental variables to predict grebe density meant that an alternative approach had to be adopted. This was based on the assumption that the surveyed grid squares within each zone were representative of Red-necked Grebe densities across the whole of each zone. Population estimates and bird densities were calculated directly from the survey

data (including correction for distance sampling where data had been collected across more than a single distance band, as in the main analysis above). The Red-necked Grebe densities (derived directly from the 2020-21 aerial surveys, hence the gaps in coverage) are mapped in Figure 5-16.

Further analysis of the Red-necked Grebe data was undertaken to test if their numbers were consistent in areas between years. If that were the case, then the grid square densities from the two years (2014-15 and 2020-21) would be expected to be correlated. There was statistically significant correlation between Red-necked Grebe densities in 2014-15 and 2020-21 (r_s =0.16, p=0.002, n=507), suggesting that they were showing some preference for similar areas between years, but this relationship was weak, probably reflecting variability in their primary food resource (fish).

Omo Syd Wind Farm: Bird Modelling Study

FIGURE 5-15

Common Eider densities and potential SPA exclusion

KEY:

Omo Syd SPA Exclusion

Eider density/sq km

0.0
0.1 - 3.5
3.6 - 10.0
10.1 - 20.0
20.1 - 35.2
35.3 - 40.0
40.1 - 58.3
58.4 - 250.0
250.1 - 500.0

Proposed SPA

Omo Syd wind farm

Existing SPAs

N/A

N/A

N/A

SCALE - 1:165,000 @ **A3**

OMO SYD WIND FARM
BIRD MODELLING STUDY
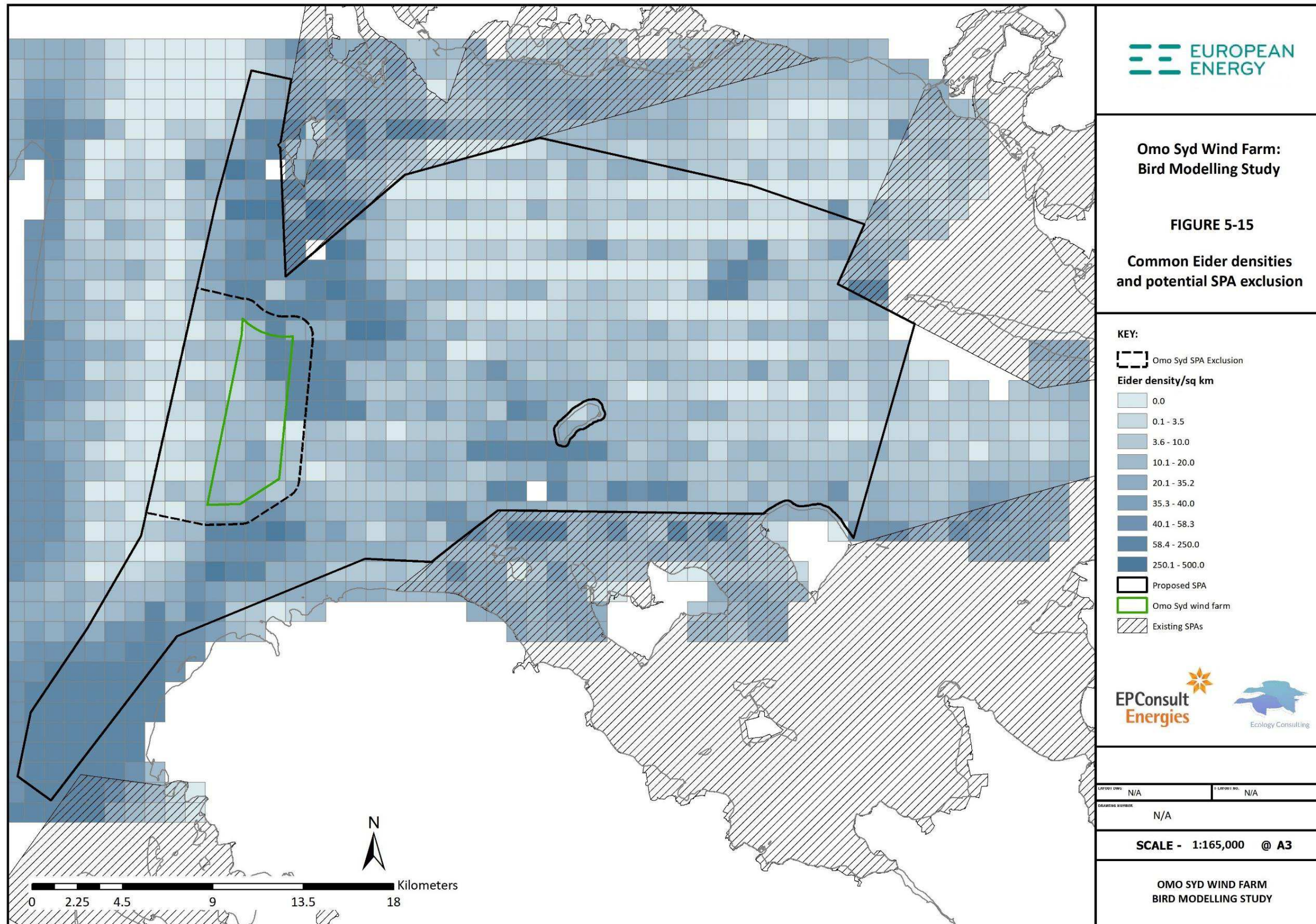
Figure 5-15: Common Eider: density surface model

EPConsult Energies

EUROPEAN ENERGY

**Omo Syd Wind Farm:
Bird Modelling Study**

FIGURE 5-16

**Red-necked Grebe:
survey densities 2020-21**

KEY:

Bird density/sq km

	0.0
	0.010 - 0.30
	0.31 - 0.70
	0.71 - 1.5
	1.6 - 3.0
	3.1 - 5.0
	5.1 - 8.0

Proposed SPA

Potential exclusion from SPA

Omo Syd wind farm

Existing SPAs

EPConsult Energies

Ecology Consulting

N

SCALE - 1:175,000 @ A3

**OMO SYD WIND FARM
BIRD MODELLING STUDY**

THIS DRAWING IS THE PROPERTY OF ECOLOGY
CONSULTING AND NO REPRODUCTION MAY BE
MADE IN WHOLE OR IN PART WITHOUT PERMISSION

Kilometers

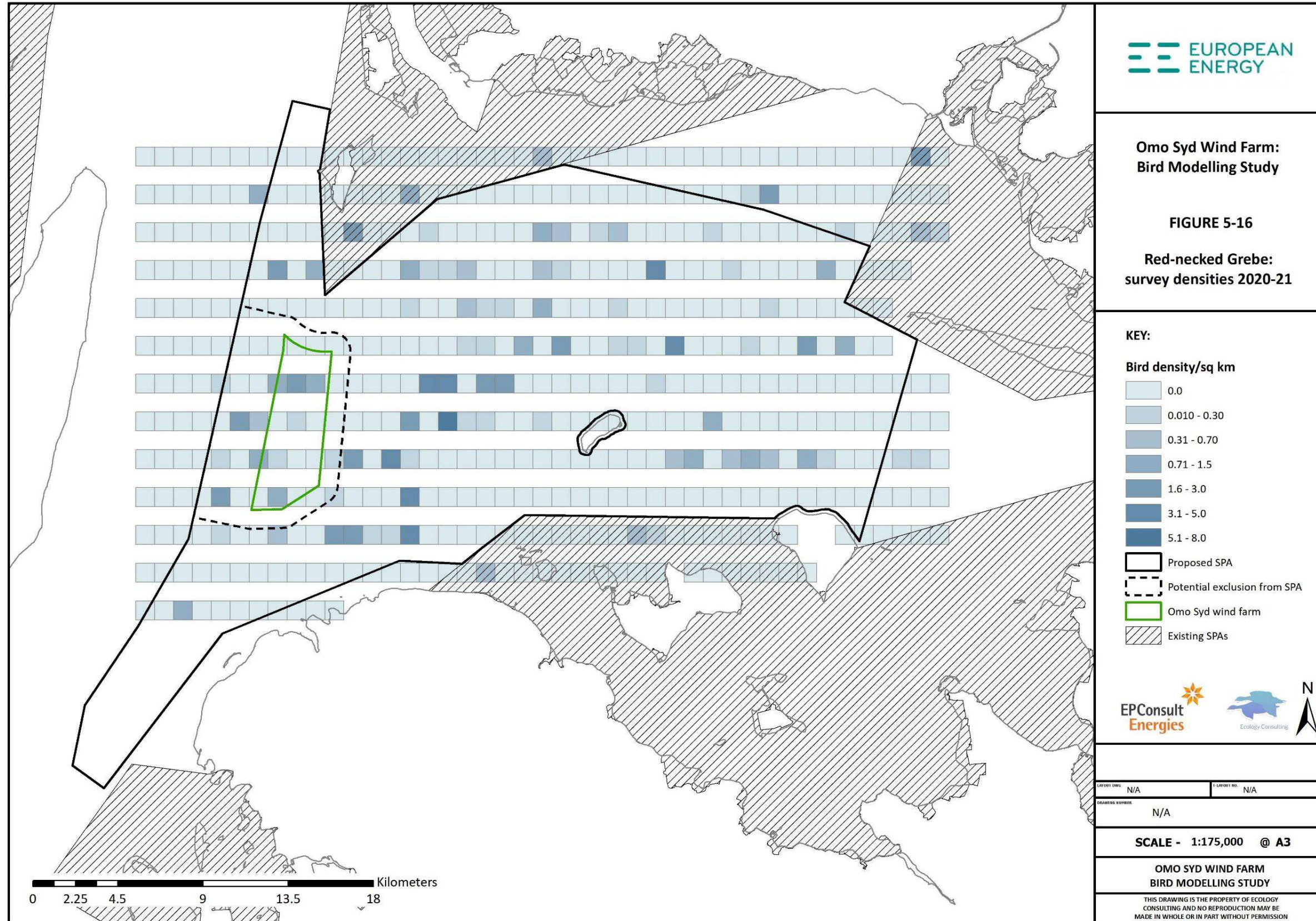0   2.25   4.5   9   13.5   18

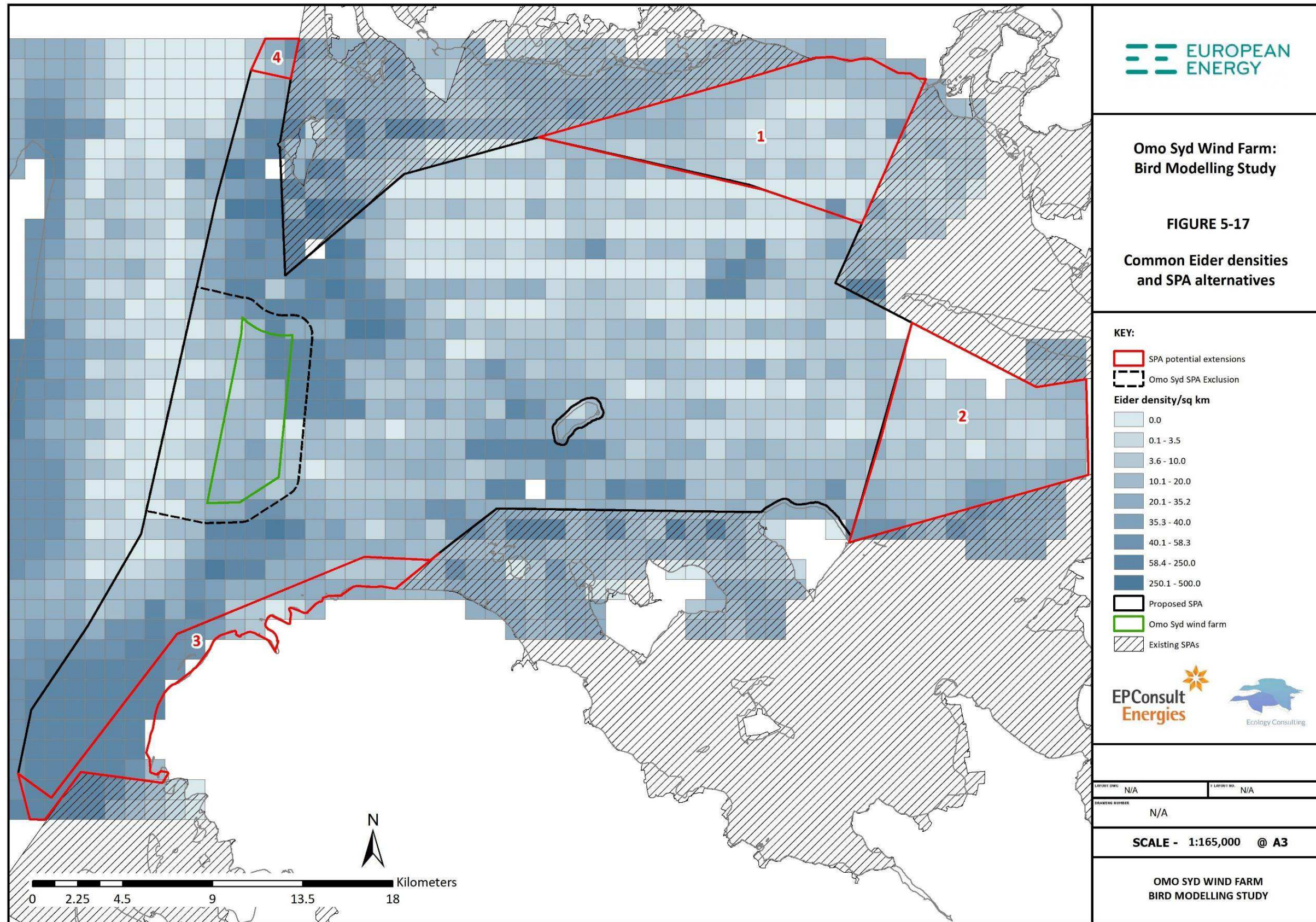**Figure 5-16: Red-necked Grebe: survey densities 2020-2021**

Figure 5-17: Wind farm options and possible SPA exclusion zones

6 Phase 3: Application of the spatial model to test the SPA alternatives

The spatial model was used to derive robust population estimates and measures of overall bird use for the proposed Special Protection Area (pSPA), and for an alternative area with the Omø Syd wind farm excluded from the pSPA. The excluded area also included a 1km buffer around the wind farm, incorporated to avoid the possibility of disturbance effects into the SPA. Additional potential SPA extensions were also investigated to see if they might offset the negative effect of the exclusion area on the SPA.

Three SPA options were therefore considered:

- Option 1 - SPA as current proposed boundary
- Option 2 - SPA with exclusion area around current wind farm location;
- Option 3 - SPA with exclusion area and alternative potential SPA extension areas..

These options are mapped in Figure 5-17.

The aim of this phase of the work was to determine how many Common Eider and Red-necked Grebe each of the SPA alternatives would support, and hence what the proportionate reduction would be in the SPA Eider and Red-necked Grebe populations for the Option 2 and Option 3 alternatives.

The modelling data were also used to determine whether removing the wind farm area from the SPA makes a material difference to the overall quality of the SPA, in terms of its ability to achieve its threshold population and to deliver and maintain its conservation objectives (for each of the two alternative options).

The contribution from each of the four possible extension areas is shown in the Table.

Table 6-1 summarises the modelled Common Eider population sizes and densities within the pSPA options. The key comparisons are the Common Eider populations for each of the options, and the proportionate change that this represents from the current pSPA. Option 2, with the wind farm and a 1km buffer excluded from the SPA would result in a reduced total SPA mean population (20,711 compared with 22,531), but this would still represent about 91.9% of the current pSPA.

The alternative Option 3 with the wind farm exclusion but also with four potential extensions to the SPA gave a predicted net gain to the Common Eider SPA population, with the updated SPA predicted to hold a mean population of 23,960 (106.3% of the current pSPA). The contribution from each of the four possible extension areas is shown in the Table.

Table 6-1: Common Eider population estimates and densities for each of the SPA options

Option	Mean population	Mean density	Sample size	% current pSPA
Option 1: current pSPA	22,531	33.3	677	100%
Option 2: pSPA with Omø Syd Wind Farm exclusion	20,711	34.2	605	91.9%
Effective loss	1,820		72	-8.1%
Extension 1 gain	766	9	81	+3.4%
Extension 2 gain	908	19	77	+4.0%
Extension 3 gain	1,500	43	35	+6.7%
Extension 4 gain	75	22	3.4	+0.3%
Total potential gain (1-4)	3,249			+14.4%
Option 3: All extensions combined + Option 2	23,960	33.6	712	106.3%

Table 6-2 summarises the estimated Red-necked Grebe population sizes and densities within the three pSPA options. As for Common Eider, the key comparisons are the Red-necked Grebe populations for each

of the three options, and the proportionate change that this represents from the current pSPA. Option 2, with the wind farm and a 1km buffer excluded from the SPA would result in a reduced total SPA population (145 compared with 165), which would represent about 87.9% of the current pSPA.

For reference, the threshold of international importance given in the pSPA documentation (Petersen *et al.* 2016 and 2019) for Red-necked Grebe is 500 (though with the flyway population estimated at 30,000-45,000). The Red-necked Grebe populations derived from the recent aerial surveys fall well below this threshold. Option 2 reduced the grebe numbers to 87.9% of the current pSPA levels. From the information provided in Petersen *et al* 2016, 2019 and 2020, it appears to be being suggested that ship-based surveys produce rather higher populations estimates for this species (with about 1,110-1,900 individuals reported from surveys in 2014). With problems of species identification and this apparent under-recording of this species from aerial surveys, it is difficult to draw any firm conclusions for Red-necked Grebe, though the available evidence would suggest that the additional exclusion areas would reduce the grebe numbers supported within the SPA by 12.1%.

Table 6-2: Red-necked Grebe population estimates and densities for each of the SPA options

Option	Mean count	Mean density	Standard error	Sample size	% current pSPA
Option 1: current pSPA	165	0.244	0.042	677	100.0%
Option 2: pSPA w/o current Omo Syd WF	145	0.240	0.046	280	87.9%

The possible SPA extensions have the potential to support small numbers of Red-necked Grebe, and probably sufficient to offset the reduction from excluding the wind farm from the SPA (given the large overall total area in comparison with the area lost to the exclusion), but it was not possible to quantity this using spatial modelling, as the model was not sufficiently reliable (primarily due to the limitations of the baseline data).

7   Summary and Conclusions

This study has provided a quantitative comparison of the numbers of the two qualifying species (Common Eider and Red-necked Grebe) within the two SPA option areas that were being investigated: (a) the current proposed designation, and (b) an alternative designation with the wind farm and a buffer excluded from SPA. A third option was also identified during the study, with the wind farm exclusion and four possible SPA extensions also considered to offset the effect of the exclusion area.

Analysis of the aerial bird survey data has enabled bird densities to be estimated across the survey area, and, for Common Eider, this has been developed with a spatial autoregression model to predict bird densities in areas of the SPA that have not been surveyed (on the basis of a range of environmental variables including the suitability of the seabed conditions to support filter-feeding bivalves, distance from shore, water depth, current speed, seabed sediment type and shipping activity).

Removing the wind farm area from the SPA (Option 2) made no material difference to the overall quality of the SPA, in terms of its ability to achieve its threshold population and to deliver and maintain its conservation objectives. The SPA would considerably exceed the threshold population of 9,800 individuals for all three options. Comparing the proportionate change in Common Eider populations, the wind farm in its current position (plus a 1km buffer) excluded from the SPA (Option 2) would result in a reduced total SPA population to about 91.9% of the current pSPA. The alternative option with the wind farm exclusion but also the SPA extensions (Option 3) would result in a net gain for the Common Eider SPA population to 106% of the current pSPA. For Red-necked Grebe, Option 2, would result in a reduction to 87.9% of the current pSPA population. Quantification of the benefits of the possible SPA extensions was not possible given the limitations of the baseline survey data, but it is very likely that this combination of exclusion and extension areas would allow the SPA Red-necked Grebe population to achieve its required conservation status (exceeding the threshold for designation and meeting its conservation objectives).

The initial recommendation would be to exclude the current proposed wind farm site and a 1km buffer from the pSPA, as shown in Figure 5-17. This would result in an 8.1% reduction in the SPA Common Eider population, and a 12.1% reduction in its Red-necked Grebe population.

An alternative option was identified, to extend the SPA to include additional areas and offset the reduction from the wind fam exclusion. Four possible SPA extensions were identified, which together could deliver a 6% increase in the SPA population of Common Eider in combination with the proposed wind farm exclusion. Such an approach would also likely offset the reduction in the Red-necked Grebe population within the SPA as a result of the proposed wind farm exclusion.

8 References

Diederichs, A., Nehls, G. & Petersen, I. K. 2002. Flugzeugzählungen zur großflächigen Erfassung von Seevögeln und marinen Säugern als Grundlage für Umweltverträglichkeitsstudien im Offshorebereich. Seevögel, 23: 38-46.

Kahlert, J., Desholm, M., Clausager, I. & Petersen, I.K. 2000. Environmental impact assessment of an offshore wind park at Rodsand: Technical report on birds. NERI Report: 86pp.

Petersen, I.K., Nielsen, R.D. & Clausen, P. 2016. Assessment of IBA (Important Bird Areas) in relation to bird protection areas - with particular reference to marine species and areas. Aarhus University, DCE - National Centre for Environment and Energy, 98 pp. - Technical report from DCE - National Centre for Environment and Energy No. 202 http://dce2.au.dk/pub/TR202.pdf

Petersen, I.K., Nielsen, R.D. & Clausen, P. 2019. Updated assessment of IBA designations in relation to eight specific marine areas. Aarhus University, DCE - National Centre for Environment and Energy, 80 pp. - Technical Report No. 203 http://dce2.au.dk/pub/TR203.pdf

Petersen, IK 2020. Academic contribution regarding. designation of marine bird protection areas. Aarhus University, DCE - National Centre for Environment and Energy, 25 pp. - - Note No 2020 | 19 https://dce.au.dk/fileadmin/dce.au.dk/Udgivelser/Notater_2021/N2020_19.pdf

Skov, H. et al. 2012. MOPODECO. Modelling of the Potential coverage of habitat forming species and Development of tools to evaluate the Conservation status of the marine Annex I habitats. TemaNord 2012:532. ISBN 978-92-893-2368-0. http://dx.doi.org/10.6027/TN2012-532. Nordic Council of Ministers 2012.

StataCorp. 2021. Stata: Release 17. Statistical Software. College Station, TX: StataCorp LLC.